INTERNATIONAL JOURNAL FOR NUMERICAL METHODS IN FLUIDS
Int. J. Numer. Meth. Fluids 2009; **59**:333–354
Published online 27 November 2007 in Wiley InterScience (www.interscience.wiley.com). DOI: 10.1002/fld.1686

A review of *a posteriori* error control and adaptivity for approximations of non-linear conservation laws

Mario Ohlberger*, †

Institut für Numerische und Angewandte Mathematik, Universität Münster, Einsteinstrasse 62, 48149 Münster, Germany

SUMMARY

In this contribution we give an overview on recent progress in obtaining *a posteriori* error control for finite volume and discontinuous Galerkin approximations of non-linear hyperbolic conservation laws. The theory is based on the celebrated doubling of variables technique introduced by Kružkov (*Math. USSR Sb.* 1970; **10**:217–243). *A posteriori* error control is of particular importance as it can be used for designing efficient grid adaptive schemes. The derivation of such adaptive methods is discussed and numerical experiments are given. Copyright © 2007 John Wiley & Sons, Ltd.

Received 9 May 2006; Revised 12 September 2007; Accepted 14 October 2007

KEY WORDS: *a posteriori* error estimates; finite volume method; discontinuous Galerkin; hyperbolic conservation laws; adaptive schemes

1. INTRODUCTION

In this paper, we are going to review the victory of Kružkov's doubling of variables technique (see [1, 2]) for obtaining rigorous *a posteriori* error control for approximations of non-linear conservation laws. As a prototype balance law, consider the Cauchy initial value problem

$$\partial_t u + \nabla \cdot F(u) = 0 \quad \text{in } \mathbb{R}^d \times \mathbb{R}^+ \tag{1}$$

$$u(\cdot, 0) = u_0 \quad \text{in } \mathbb{R}^d \tag{2}$$

Here $u: \mathbb{R}^d \times \mathbb{R}^+ \to \mathbb{R}$ denotes the dependent solution variable, $F \in C^1(\mathbb{R})$ the flux function, and $u_0 \in \mathrm{BV}(\mathbb{R}^d) \cap L^\infty(\mathbb{R}^d)$ the initial data with $u_0 \in [A, B]$ a.e. In this presentation we restrict ourselves to the conservation law (1) without source terms, although also more general situations may be considered (see [3]).

*Correspondence to: Mario Ohlberger, Institut für Numerische und Angewandte Mathematik, Universität Münster, Einsteinstrasse 62, 48149 Münster, Germany.
†E-mail: mario.ohlberger@uni-muenster.de

It is well known that, in general, classical solutions to problem (1)–(2) do only exist for finite time, even when the initial data u_0 are arbitrarily smooth. On the other hand, weak solutions are not uniquely defined by their initial data and therefore we have to work in the L^1-framework of entropy solutions [4], i.e. with weak solutions that satisfy a Kružkov–Vol'pert type entropy condition. In this paper we will use the definition of an entropy weak solution as introduced in [5].

Definition 1.1 (*Entropy weak solution*)
Let u be a weak solution of (1)–(2). Then, u is called an entropy weak solution if u satisfies for all entropy pairs (S, F_S)

$$\int_{\mathbb{R}^d}\int_{\mathbb{R}^+}(S(u)\partial_t\phi + F_S(u)\cdot\nabla\phi)\,\mathrm{d}t\,\mathrm{d}x + \int_{\mathbb{R}^d} S(u_0)\phi(x,0)\,\mathrm{d}x \geqslant 0 \tag{3}$$

for all $\phi \in C_0^1(\mathbb{R}^d \times \mathbb{R}^+, \mathbb{R}^+)$.

Recall that (S, F_S) is called an entropy–entropy flux pair or more simply an entropy pair for Equation (1), iff S is convex and $F_S' = S' f'$.

The theory that we will present in this contribution is based on the doubling of variables technique introduced in the pioneering work of Kružkov [1] where uniqueness of solutions of scalar conservation laws was shown, i.e. we will work with the family of Kružkov entropies $S(u) = |u-\kappa|, \kappa \in \mathbb{R}$ or with smooth approximations of these. For hyperbolic boundary value problems, the theory was later on generalized. We refer for instance to the work of Otto [6] and Vovelle [7].

In the context of *a priori* error estimates for approximations of scalar conservation laws, the doubling of variables technique is meanwhile broadly used. See, for example, [8–15].

Unfortunately, *a priori* error estimates mainly give information on the asymptotic convergence behavior of the approximation scheme but do not provide an error control, as the exact solution and therefore the constants appearing in the error estimates are not known *a priori*. Hence, for error control, it is necessary to derive *a posteriori* error estimates of the form

$$\|u - u_h\| \leqslant \eta_h(u_h) + A_h \tag{4}$$

where the indicator η_h denotes a computable quantity that only depends on the approximated solution u_h, and A_h stands for data approximation errors.

Cockburn and Gau [16] were probably one first in noticing that the doubling of variables technique provides in a natural way estimates of type (4). An additional input towards local error estimates for hyperbolic conservation laws was provided by Eymard *et al*. [10] and Chainais–Hillairet [15]. They proved that the error in a given space–time domain can be estimated in terms of its history in the domain of dependence. This idea was then used in [3] to obtain local *a posteriori* error estimates for scalar conservation laws, which were proved to provide a good basis for designing efficient adaptive solution strategies for the underlying finite volume method.

The rest of the paper is organized as follows. In Section 2 we will discuss the basic approach in obtaining *a posteriori* error control for approximation of (1)–(2) within the framework of Kružkov's doubling of variables technique. In Section 3 we will state the *a posteriori* error estimate for finite volume approximations obtained in [3] for the initial value problem. Concerning initial boundary value problems, an *a posteriori* result was recently obtained in [17]. We will give a review of this result in Section 4. Finally, in Section 5 we state a result on error control for an hp-adaptive Runge–Kutta discontinuous Galerkin CRK-DG, method of higher order that was recently obtained in [18]. This result is of special importance as it guarantees a numerical error control for a scheme

DOI: 10.1002/fld

where we do not know any convergence result or *a priori* error estimate. Finally, in Section 6 we describe how *a posteriori* error control can be used to design efficient grid adaptive algorithms. Some numerical experiments underline the benefits of the resulting adaptive schemes. A section on a discussion of further results concludes the paper (see Section 7).

2. GENERAL CONCEPT FOR OBTAINING ERROR CONTROL

We introduce a general approach for obtaining error control for approximations of scalar conservation laws. The approach is based on the doubling of variables technique of Kružkov (see [1, 2]). In essence, this technique enables one to estimate the error between the exact solution u and approximate solution u_h of a conservation law in terms of the entropy residual $R_S(u_h)$ which is defined as follows.

Definition 2.1 (*Entropy residual* R_S)
Let $v \in L^\infty(\mathbb{R}^d \times \mathbb{R}^+)$ be an arbitrary function. Then, corresponding to the definition of an entropy weak solution, we define the entropy residual R_S by

$$\langle R_S(v), \phi \rangle := \iint_{\mathbb{R}^d \times \mathbb{R}^+} S(v)\partial_t \phi + F_S(v) \cdot \nabla \phi + \int_{\mathbb{R}^d} S(u_0)\phi(\cdot, 0) \tag{5}$$

The following theorem gives a fundamental error estimate for conservation laws independent of the particular finite volume scheme (see [3, 14, 15]).

Theorem 2.2 (*Fundamental error estimate*)
Let $u_0 \in BV(\mathbb{R}^d)$ and let u be an entropy weak solution of (1)–(2). Furthermore, let $v \in L^\infty(\mathbb{R}^d \times \mathbb{R}^+)$ be an arbitrary function and let us denote by $S(u) := |u - \kappa|$ the Kružkov entropy. Suppose that there exist measures $\mu_v \in \mathscr{M}(\mathbb{R}^d \times \mathbb{R}^+)$ and $\nu_v \in \mathscr{M}(\mathbb{R}^d)$ such that R_S can be estimated independently of κ by

$$\langle R_S(v), \phi \rangle \geqslant -(\langle |\partial_t \phi| + |\nabla \phi|, \mu_v \rangle + \langle |\phi(\cdot, 0)|, \nu_v \rangle) \tag{6}$$

Let $K \subset\subset \mathbb{R}^d \times \mathbb{R}^+$, $\omega \equiv \mathrm{Lip}(f)$, and choose T, R and x_0 such that $T \in]0, \frac{R}{\omega}[$ and K lies within its cone of dependence D_0, i.e. $K \subset D_0$ where D_δ is given as

$$D_\delta := \bigcup_{0 \leqslant t \leqslant T} B_{R-\omega t+\delta}(x_0) \times \{t\} \tag{7}$$

Then, there exist a $\delta \geqslant 0$ and positive constants C_1, C_2 such that u, v satisfy the following error estimate:

$$\|u - v\|_{L^1(K)} \leqslant T(\nu_v(B_{R+\delta}(x_0)) + C_1 \mu_v(D_\delta) + C_2 \sqrt{\mu_v(D_\delta)}) \tag{8}$$

The error estimate (8) can be used either as an *a posteriori* control of the error, as the right-hand side only depends on v, or it can be used as an *a priori* error bound if one is able to estimate further the measures μ_v and ν_v using some *a priori* bounds on v. Finally, note that comparable estimates to (8) are obtainable in the $L^\infty(0, T; L^1(\mathbb{R}^d))$-norm (see [16, 18–20]). The proof of Theorem 2.2 relies on the doubling of variables technique of Kružkov and can be found in [3, 14, 15].

With the fundamental error estimate in hand, the main ingredient in obtaining a computable error control for approximations of (1)–(2) is an explicit knowledge of the measures μ_v, ν_v that can be

DOI: 10.1002/fld

obtained by estimating the entropy residual R_S. In the case of finite volume approximations with monotone flux functions such an estimate on the entropy residual can be obtained by exploiting the discrete entropy inequality that is satisfied by the discrete solution (see [3]). We will state the resulting *a posteriori* error estimate in the following section.

3. CELL CENTERED FINITE VOLUME APPROXIMATIONS

Let $\mathscr{T}=\{T_j \mid j\in J\}$ be a mesh of $\mathbb{R}^d$ such that the interface of two neighboring cells T_j, T_l of $\mathscr{T}$ is included in a hyperplane (see also [3]). The joint edge of T_j and T_l will be denoted by S_{jl}. We assume that there exists an $\alpha>0$ such that we have for all $h_j:=\mathrm{diam}(T_j)$

$$\alpha h_j^d \leqslant |T_j|, \quad \alpha|\partial T_j| \leqslant h_j^{d-1} \tag{9}$$

for all $j,l\in J$. Moreover, we define $h:=\max_{j\in J} h_j$ and $h_{\min}:=\min_{j\in J} h_j$. We denote by $\{t^n \mid n\in I\}, I:=\{0,\ldots,N\}$ a discretization of the time interval $[0,T]$ with local step sizes $\Delta t^n := t^{n+1}-t^n$.

For the numerical fluxes f_{jl}, we impose the following assumption.

Assumption 3.1 (*Monotone numerical flux function*)
The numerical fluxes are supposed to be functions $f_{jl}\in C^1(\mathbb{R}^2,\mathbb{R})$ that satisfies for all $u,v,u',v'\in[A,B]$ the following conditions (monotony, conservation, regularity, consistency):

$$\partial_u f_{jl}(u,v)\geqslant 0, \quad \partial_v f_{jl}(u,v)\leqslant 0, \quad f_{jl}(u,v)=-f_{lj}(v,u) \tag{10}$$

$$f_{jl}(u,u)=n_{jl}|S_{jl}|F(u), \quad |f_{jl}(u,v)-f_{jl}(u',v')|\leqslant L S_{jl}|(|u-u'|+|v-v'|) \tag{11}$$

where n_{jl} denotes the outer unit normal to S_{jl}.

With this notation, the cell centered upwind finite volume scheme for computing approximate solutions to (1)–(2) is defined by following definition.

Definition 3.2 (*Finite volume scheme*)
Let

$$u_j^0 := \frac{1}{|T_j|}\int_{T_j} u_0, \quad u_j^{n+1} := u_j^n - \frac{\Delta t^n}{|T_j|}\sum_{l\in N(j)} f_{jl}(u_j^n,u_l^n) \tag{12}$$

for all $n\in N(j)$ and $j,l\in J$ where $N(j)$ denotes the indices of all neighboring triangles of T_j. The piecewise constant approximate solution u_h is then given by

$$u_h(x,t) := u_j^n \quad \text{if } x\in T_j, \quad t^n < t \leqslant t^{n+1} \tag{13}$$

The stability of this explicit scheme is ensured under the following CFL-condition (see [3] and the references therein).

Assumption 3.3 (*CFL-condition*)
We assume the following CFL-condition, for a given $\xi\in(0,1)$:

$$\Delta t^n \leqslant \frac{(1-\xi)\alpha^2 h_{\min}^n}{L}$$

where L is the Lipschitz constant from (11).

DOI: 10.1002/fld

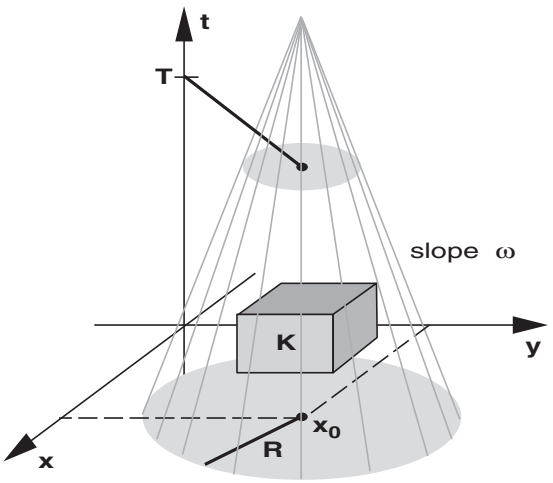

Figure 1. Notation and cone of dependence for hyperbolic conservation laws.

The stability condition for the explicit finite volume scheme says that the time step size has to be chosen proportional to the smallest mesh size. This may lead to very small time steps, if mesh adaptivity is considered. A possible solution to this is the introduction of local time step sizes in space. However, if the major part of the computational grid cells are on the finest grid level, the computational costs for both approaches are approximately the same.

Let u be the exact solution of (1)–(2) and u_h be the discrete solution as defined in (13). In [8–10, 15] it was shown that under the assumption mentioned above we have for any compact set $K \subset \mathbb{R}^d \times \mathbb{R}^+$

$$\int_K |u(x,t) - u_h(x,t)| \, \mathrm{d}x \, \mathrm{d}t \leqslant c h^{1/4} \tag{14}$$

where the constant c depends only on K and the given data.

In order to present the corresponding *a posteriori* error estimate in the case $d=2$, we define for given R, ω, T (recall the definition of D_{R+1} through (7)):

$$I_0 := \left\{ n \,|\, 0 \leqslant t^n \leqslant \min\left\{ \frac{R+1}{\omega}, T \right\} \right.$$

$$M(t) := \{ j \,|\, \text{there exists } x \in T_j \text{ such that } (x,t) \in D_{R+1} \}$$

Theorem 3.4 (*Kröner and Ohlberger* [*3*])
Assume the conditions as mentioned above and $u_0 \in BV(\mathbb{R}^2)$. Let $K \subset\subset \mathbb{R}^2 \times \mathbb{R}^+$, $\omega \equiv \mathrm{Lip}(f)$ and choose T, R and x_0 such that $T \in]0, \frac{R}{\omega}[$ and $K \subset D_0$ (see Figure 1). Then, we have

$$\int_K |u - u_h| \leqslant T a_0 \left[\int_{|x-x_0|<R+1} |u_0 - u_h(\cdot,0)| + a Q + 2\sqrt{bQ} \right] \tag{15}$$

DOI: 10.1002/fld

where

$$Q := \sum_{n\in I}\sum_{j\in M(t^n)} \Delta t^n h_j^2 |u_j^{n+1} - u_j^n| + 2L\Delta t^n \sum_n \sum_{E(t_n)} (\Delta t^n + h_{jl}) h_{jl} |u_j^n - u_l^n|)$$

and $E(t_n)$ is the set of all edges that lie in $M(t^n)$. In the sum over $E(t_n)$, the indices j, l refer to the triangles T_j, T_l such that $T_j \cap T_l$ is the corresponding edge and $h_{jl} := \operatorname{diam}(T_j \cup T_l)$.

The constants a_0, a, and b are explicitly known. A corresponding result also holds in $\mathbb{R}^d$ with $d > 2$. Under suitable conditions this theorem can be generalized if we replace $F(u)$ by $F(x, t, u)$ (see [3]).

4. ERROR CONTROL FOR BOUNDARY VALUE PROBLEMS

Although the study of the finite volume method applied to the Cauchy problem (1)–(2) has led to the understanding of most of the mechanisms that govern the accuracy of this numerical method, the initial-boundary value problem (see (16)–(18) below) is even of greater importance in applications, and its approximation by finite volume schemes deserves an analysis.

A new difficulty for boundary value problems is that boundary values may be prescribed only at *outflow boundaries* that themselves depend on the solution of the problem. This feature leads to a more involved theory for the error analysis and, in addition, may lead to a creation of artificial boundary layers of the finite volume approximation. In the sequel we consider an implementation of boundary data *via* 'ghosts control volumes' (see Figure 2). This is a way to compute the numerical fluxes at the boundary of the domain inspired by the design of the fluxes inside the domain. This method of computation of the numerical fluxes at the boundary is classical and ensures the convergence of the finite volume scheme to the entropy solution of problem (16)–(18) (see [7, 21–23]).

Let Ω be an open convex polygonal bounded domain in $\mathbb{R}^d$, $d = 2, 3$ and let $T \in \mathbb{R}^+$. We consider the following initial boundary value problem for non-linear scalar conservation laws:

$$u_t + \nabla \cdot F(u) = 0 \quad \text{in } \Omega \times (0, T) \tag{16}$$

$$u(\cdot, 0) = u_0 \quad \text{in } \Omega \tag{17}$$

$$u(x, t) = \overline{u}(t, x) \quad \text{in } \partial\Omega \times (0, T) \tag{18}$$

The flux in Equation (16) is given by the function $F \in \mathscr{C}^1(\mathbb{R}; \mathbb{R}^d)$; the functions $u_0 \in L^\infty(\Omega)$ and $\overline{u} \in L^\infty(\partial\Omega \times (0, T))$ are, respectively, the initial and boundary data of the problem (16)–(18).

Of course the boundary condition in problem (16)–(18) has to be understood in a specific sense. For general flux F and in the context of entropy solutions, problem (16)–(18) has first been analyzed by Bardos *et al.* [24] in the BV framework. The notion of entropy solution given there has been extended, in the L^∞ setting, by Málek *et al.* [25] and Otto [6]. We use this last definition and define the following semi Kružkov entropy pairs [26, 27].

Definition 4.1 (*Semi Kružkov entropy pairs*)
Set $v^+ = \max\{v, 0\}$, $v^- = (-v)^+$. We denote by $F_{S_\kappa^\pm}(v)$ the entropy flux associated with the entropy $S_\kappa^\pm(v) := (v - \kappa)^\pm$.

DOI: 10.1002/fld

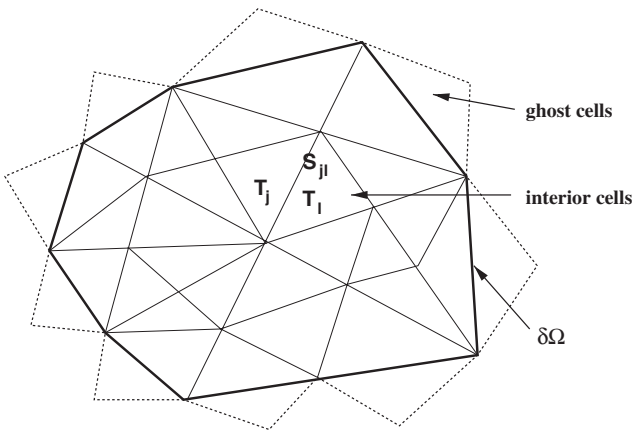

Figure 2. The concept of ghost cells and notation for the grid.

We further denote by $A, B \in \mathbb{R}$ some lower and upper bounds for the data, i.e. $A \leqslant u_0, \overline{u} \leqslant B$ a.e. We set $\mathscr{C} = \max(|A|, |B|)$, and let $\mathscr{L}$ be a fixed real satisfying

$$\max\{|F'(v)|;\ v \in [A, B]\} \leqslant \mathscr{L} \tag{19}$$

Then the unique entropy weak solution to the initial-boundary value problem (16)–(18) is defined as follows (see [7]).

Definition 4.2 (*Entropy weak solution*)
A function $u \in L^\infty(\Omega \times (0, T))$ is called an entropy weak solution of (16)–(18) if it satisfies the following entropy inequalities: for all $\kappa \in [A, B]$, for all $\varphi \in C_0^\infty(\mathbb{R}^d \times \mathbb{R}^+)$ with $\varphi \geqslant 0$:

$$\int_{\Omega\times(0,T)} S_\kappa^\pm(u)\partial_t\varphi + F_{S_\kappa^\pm}(u)\cdot\nabla\varphi + \int_\Omega S_\kappa^\pm(u_0)\varphi(\cdot,0) + \mathscr{L}\int_{\partial\Omega\times(0,T)} S_\kappa^\pm(\overline{u})\varphi \geqslant 0 \tag{20}$$

Let us introduce some notation for the definition of the ghost cells and the resulting finite volume scheme (see Figure 2). The set of internal edges $\mathscr{S}_{\text{int}}^n$ and the oriented set of internal edges $\mathscr{E}_{\text{int}}^n$ are defined as

$$\mathscr{S}_{\text{int}}^n := \{\{(j,l) \in J_{\text{int}}^n \times J_{\text{int}}^n\} | S_{jl} \text{ interior edge of } \mathscr{T}^n\}, \quad \mathscr{E}_{\text{int}}^n := \{(j,l) \in \mathscr{S}_{\text{int}}^n | j > l\}$$

Let the index set of ghost cells J_{ext}^n be such that $J_{\text{ext}}^n \cap J_{\text{int}}^n = \emptyset$ and such that for each edge $S \subset \partial\Omega$ there exists a unique pair of indices $(j,l) \in J_{\text{int}}^n \times J_{\text{ext}}^n$ with $\partial T_j \cap S = S$. In this situation we denote $S_{jl} := S$. Accordingly, the set of edges located on the boundary of Ω is defined by

$$\mathscr{S}_{\text{ext}}^n := \{(j,l) \in J_{\text{int}}^n \times J_{\text{ext}}^n | S_{jl} \text{ exterior edge of } \mathscr{T}^n\}$$

With this notation we define the finite volume schemes on bounded domains.

DOI: 10.1002/fld

Definition 4.3 (*Finite volume scheme*)
Set

$$u_j^0 := \frac{1}{|T_j|}\int_{T_j} u_0, \quad j \in J_{\text{int}}^0, \qquad u_l^n := \frac{1}{\Delta t}\frac{1}{|S_{jl}|}\int_{t^n}^{t^{n+1}}\int_{S_{j,l}} \overline{u}(x,t)\,\mathrm{d}x\,\mathrm{d}t, \quad (j,l) \in \mathscr{S}_{\text{ext}}^n$$

The discrete evolution of the approximation u_j of u on the cell T_j is governed by

$$u_j^{n+1} := c_j^n - \frac{\Delta t^n}{|T_j|}\sum_{l \in N(j)} f_{jl}^n(u_j^n, u_l^n), \quad j \in J_{\text{int}}^n \tag{21}$$

for all $n \in \{0, \ldots, N\}$ where $N(j)$ now also includes the neighboring ghost indices across the boundaries of the domain Ω. Given u_j^n, we define the approximate solution $u_h : \Omega \times (0,T) \to \mathbb{R}$ by

$$u_h(x,t) := u_j^n \quad \text{if } x \in T_j, \quad t^n \leqslant t < t^{n+1} \tag{22}$$

We are now prepared to state the *a posteriori* error estimate for the finite volume approximation.

Theorem 4.4 (*A posteriori error estimate Ohlberger and Vovelle* [*17*])
Let u_h be the discrete solution defined in Definition 4.3 and u the entropy solution of (16)–(18). Furthermore, let Assumptions 3.1 and 3.3 be fulfilled. Then the following error estimate holds

$$\|u_h - u\|_{L^1(\Omega\times(0,T))} \leqslant \eta(u_h) \tag{23}$$

with

$$\eta(u_h) := 2T(N_f+1)\min_{\varepsilon,\delta\in\mathbb{R}^+}\left[\eta_0 + \overline{\eta} + (\eta_t+\eta_c)K_1\varepsilon + \eta_c K_1'(\varepsilon+\delta) + K_0\left(\frac{2}{\varepsilon}+\frac{\varepsilon}{\delta}\right)\right]$$

Here the indicators η_0, η_t, η_c, and $\bar{\eta}$ are defined by

$$\eta_0 = \int_{\mathbb{R}^d} |u_h(x,0) - u_0(x)|\,\mathrm{d}x, \quad \eta_t = \sum_n \sum_{j\in J^n} |T_j|\Delta t^n |u_j^{n+1} - u_j^n|$$

$$\eta_c = \sum_n \sum_{(j,l)\in\mathscr{E}^n}\left[2(h_{jl}+\Delta t^n)\Delta t^n\left(\max_{u_l^n \leqslant a \leqslant b \leqslant u_j^n}(f_{jl}^n(b,a) - f_{jl}^n(b,b))\right.\right.$$

$$\left.\left. + \max_{u_l^n \leqslant a \leqslant b \leqslant u_j^n}(f_{jl}^n(b,a) - f_{jl}^n(a,a))\right)\right]$$

$$+ \sum_n \sum_{(j,l)\in\mathscr{S}_{\text{ext}}^n} \mathscr{L}(u_j + u_l - 2C_m)h_j \Delta t^n h_{jl}$$

$$\overline{\eta} = \int_{\partial\Omega\times(0,T)} |\overline{u}_h - \overline{u}|\,d\gamma(x)\,\mathrm{d}t$$

and the positive constants N_f, K_1, K_1', and K_2 are computable (for details see [17]).

DOI: 10.1002/fld

From the error estimate (23), we deduce an *a priori* error estimate with the following bounds on $\eta_0, \overline{\eta}, \eta_t, \eta_c$ (see [10, 15]):

$$\eta_0+\overline{\eta}+\eta_t+\eta_c\leqslant Kh^{1/2}$$

and by choosing, for example:

$$\varepsilon:=\left(\frac{(\eta_t+\eta_c)K_1+\eta_c K_1'}{K_0}\right)^{-1/3},\quad \delta:=\left(\frac{K_0 r}{\eta_c K_1'}\right)^{1/2}$$

Theorem 4.5 (*A priori error estimate Ohlberger and Vovelle* [*17*])
Let u_h be the discrete solution defined in Definition 4.3 and c the entropy solution of (16)–(18). Furthermore, let Assumptions 3.1 and 3.3 be fulfilled. Then we have for uniform meshes of mesh size h the following *a priori* error estimate

$$\|u-u_h\|_{L^1(\Omega\times(0,T))}\leqslant\eta(u_h)\leqslant Kh^{1/6} \tag{24}$$

Here, K denotes a generic constant independent of the mesh size.

Remark 4.6 (*Non-optimal order of convergence*)
The error estimates in Theorems 4.4, and 4.5 are non-optimal compared with the convergence rate $h^{1/4}$ that can be proved for finite volume approximations of the Cauchy problem (cf. [15]). Let us mention that in the special situation where $F(x,t,c)=u(x,t)f(c)$, and f is monotone, this estimate can be improved, and the order $h^{1/4}$ is recovered (see also [28]). However, the improvement in this special situation makes excessive use of the *a priori* knowledge of inflow, and outflow boundaries and gives no hint to improve general result stated above.

Note that under suitable conditions, these results on bounded domains can be generalized if we replace $F(u)$ by $F(x,t,u)$ (for details see [17]).

5. DISCONTINUOUS GALERKIN APPROXIMATIONS

A possible higher-order generalization of the finite volume method introduced in Sections 3 and 4 is the RK-DG approximation of Cockburn and Shu [29]. In the following, we analyze a generalized semi-discrete version of this method for the Cauchy problem (1)–(2). The available theory for RK-DG methods for nonlinear problems is limited to certain stability properties proved in [29, 30] and to error estimates for one-dimensional smooth solutions (see [31]). The problem of showing convergence towards the unique entropy solution for the high-order version of these methods seems rather difficult. Although a convergence result for the RK-DG method is not available, we are going to present a rigorous error control for DG methods that was recently obtained in [18].

In order to define the RK-DG methods, let us introduce further notations. On $\mathscr{T}$ we define the space of discontinuous piecewise polynomials of degree p by

$$V_h^p:=\{v_h\in BV(\mathbb{R}^d)\,|\,v_j:=v_h|_{T_j}\in\mathbb{P}_p \text{ for all } T_j\in\mathscr{T}\} \tag{25}$$

Let us denote $\Pi_{V_h^p}$ the L^2-projection into V_h^p.

The semi-discrete DG-finite element scheme is the basis of the definition of RK-DG methods.

DOI: 10.1002/fld

Definition 5.1 (*Space-discrete DG approximation*)
$u_h : C^1(0,T;V_h^p)$ is called a semi-discrete DG approximation of (1)–(2), if

$$u_h(0) = \Pi_{V_h^p}(u_0) \tag{26}$$

$$\frac{\mathrm{d}}{\mathrm{dt}}(u_j(t), v_j)_{T_j} - (F(u_j(t)), \nabla v_j)_{T_j} + \sum_{l \in N(j)} (f_{jl}(u_j(t), u_l(t)), v_j)_{S_{jl}} = 0$$

$$\text{for all } v_j \in \mathbb{P}_p, T_j \in \mathscr{T} \tag{27}$$

Here $(\cdot,\cdot)_{T_j}$ denotes the local L^2-inner product on T_j, $(\cdot,\cdot)_{S_{jl}}$ denotes the local L^2-inner product on S_{jl}, and f_{jl} is a monotone numerical flux on S_{jl} satisfying Assumption 3.1.

In the literature of DG methods, the stabilization due to the 'upwinding' of the discrete fluxes is usually accompanied by extra artificial 'shock capturing' terms as in [32–34] or limiting projections as in [29]. The RK-DG methods introduced by Cockburn and Shu are based on a combination of limiting projections and a Runge–Kutta discretization of (27). Therefore, in the next step we are going to introduce limiting projections in the discretization. To this end we associate with each time interval $(t^n, t^{n+1}]$ a (possibly different) finite element space V_h^p denoted by

$$V_{h,n}^p := \{v_h \in BV(\mathbb{R}^d) | v_h|_T \in \mathbb{P}_p \text{ for all } T \in \mathscr{T}_n\} \tag{28}$$

The associated index set of $\mathscr{T}_n$ is denoted by J^n.

To define a local projection operator, we proceed as follows: We define $\overline{v_h}$ through $\overline{v_j} := \Pi_{V_h^0}(v)|_{T_j}$ for any $v \in L^2(\Omega)$, i.e. $\overline{v_h}$ is the elementwise average of v_h. Furthermore, with each n we associate projections $\Lambda_h^{n,t}$ with the following properties.

Assumption 5.2 (*Projection operator*)
The projection $\Lambda_h^{n,t}$ is supposed to be a continuous function with respect to t on the interval $[t^n, t^{n+1}]$. If $t \in (t^n, t^{n+1}]$, the operators act $\Lambda_h^{n,t} : V_{h,n}^p \to V_{h,n}^p$ and satisfy

$$\overline{\Lambda_h^{n,t}(v_h(\cdot,t))} = \overline{v_h(t)}, \quad t \in (t^n, t^{n+1}] \tag{29}$$

In addition, $\Lambda_h^{n,t^n} : V_{h,n-1}^p \to V_{h,n}^p$ is a projection to the new mesh, still with the property

$$\overline{\Lambda_h^{n,t^n}(v_h(\cdot,t^n))} = \overline{v_h(t^n)} \tag{30}$$

In the last equation, the elementwise average is taken in the new mesh, i.e. corresponds to the projection $\Pi_{V_{h,n}^0}$. At t^n the two operators Λ_h^{n,t^n} and Λ_h^{n-1,t^n} satisfy

$$\|\Lambda_h^{n,t^n}(u_h) - \overline{u_h}\|_\infty \leqslant \|\Lambda_h^{n-1,t^n}(u_h) - \overline{u_h}\|_\infty \tag{31}$$

Properties (29), (30) lead to a conservation of mass, whereas assumption (31) guarantees that the gradients in the discrete solution are not increased between time steps. Note that $\Lambda_h^{n,t}$ accounts for both limiting projections and projections to the new spaces. We define the restriction of $\Lambda_h^{n,t}$ on the element T_j by $\Lambda_j^{n,t}$:

$$\Lambda_j^{n,t} \equiv \Lambda_h^{n,t} \quad \text{in } T_j \times [t^n, t^{n+1}], \quad j \in J^n$$

DOI: 10.1002/fld

We now define the generalized semi-discrete DG approximation.

Definition 5.3 (*Generalized semi-discrete DG approximation*)
Let us suppose that a projection $\Lambda_h^{n,t}$ with the above properties is given. In addition, assume that the discrete fluxes f_{ij} are monotone. The function u_h is called a generalized semi-discrete DG approximation of (1)–(2), if for $u_h^{-1} := \Pi_{V_{h,0}^p}(u_0)$ u_h satisfies:

For $n=0,\dots,N-1$, $u_h^n|_{[t^n,t^{n+1}]} \in C^1(t^n,t^{n+1};V_{h,n}^p)$ is defined through

$$u_h^n(t^n) := \Lambda_h^{n,t^n}(u_h^{n-1}(t^n)) \tag{32}$$

$$\frac{\mathrm{d}}{\mathrm{d}t}(u_j^n(t),v_j)_{T_j} = -\sum_{l\in N(j)}(f_{jl}(\Lambda_j^{n,t}(u_h^n(t)),\Lambda_l^{n,t}(u_h^n(t))),v_j)_{S_{jl}} + (f(\Lambda_j^{n,t}(u_h^n(t))),\nabla v_j)_{T_j}, \text{ for all } v_j\in\mathbb{P}_p,\quad j\in J^n,\quad t\in(t^n,t^{n+1}) \tag{33}$$

The global approximation $u_h \in L^\infty(0,T;V_{h,n}^p)$ is defined through $u_h(0) := u_h^{-1}$, and $u_h|_{(t^n,t^{n+1}]} := u_h^n|_{(t^n,t^{n+1}]}$.

In applications, the above method is combined with Runge–Kutta time discretizations of the ode (33) to obtain the generalized fully discrete RK-DG class of methods. This class not only includes the method of Cockburn and Shu but also alternative choices for the limiting projections that are motivated by the *a posteriori* result for (32)–(33) given follows (for more details and numerical experiments we refer to [18, 35]).

We present an *a posteriori* estimate for the error $\|(u-u_h)(T)\|_{L^1}$. To do that, we compare u and u_h with $\widetilde{u}_h$ defined as

$$\widetilde{u}_h = \Lambda_h^{n,t}u_h \quad \text{in } (t^n,t^{n+1}],\ \ n=0,\dots,N-1 \tag{34}$$

Then $\|(\widetilde{u}_h-u_h)(T)\|_{L^1}$ is an *a posteriori* quantity and the control of $\|(u-\widetilde{u}_h)(T)\|_{L^1}$ can be obtained by employing Kruzkov estimates.

Note that by definition, $\widetilde{u}_h$ might be discontinuous at the time nodes t^n. This is the case either when the spatial mesh is modified at this node or when we decide to use different projections at t^{n-1} and t^n. In fact due to the definitions of u_h and the projections, we have

$$\widetilde{u}_h(t^{n+}) - \widetilde{u}_h(t^n) = \Lambda_h^{n,t^n}u_h(t^n) - \Lambda_h^{n-1,t^n}u_h(t^n) = (\Lambda_h^{n,t^n} - \Lambda_h^{n-1,t^n})u_h(t^n) \tag{35}$$

Before stating our main result, we introduce the following notations:

$$\widetilde{u}_j = \widetilde{u}_h \text{ in } T_j, \quad \widetilde{u}^n = \widetilde{u}_h \text{ in } (t^n,t^{n+1}], \quad \widetilde{u}^n(t^n) = \widetilde{u}_h(t^{n+})$$

with the obvious extension for combined indexes.

Theorem 5.4 (*A posteriori error estimate Dedner et al.* [*18*])
Let u_h be given by the semi-discrete generalized DG method (32)–(33). For $\widetilde{u}_h$ given by (34), we have the following *a posteriori* error estimate

$$\begin{aligned}\|(u-u_h)(T)\|_{L^1(B_R(x_0))} &\leqslant \|(\widetilde{u}_h-u_h)(T)\|_{L^1(B_R(x_0))} + \|(u-\widetilde{u}_h)(T)\|_{L^1(B_R(x_0))}\\ &\leqslant \|(\widetilde{u}_h-u_h)(T)\|_{L^1(B_R(x_0))} + \eta_h\end{aligned}$$

DOI: 10.1002/fld

where $\eta_h := \eta_0 + \sqrt{K_1\eta_1} + \sqrt{K_2\eta_2}$, $\eta_0 := \sum_{j\in J^0}\eta_{0,j}$, $\eta_i := \sum_n \sum_{j\in J^n}\eta_{i,j}^n$, $i=1,2$, and the local contributions $\eta_{i,j}^n$ are given as

$$\eta_{0,j} := \int_{T_j} |u_0 - \widetilde{u}_j^0(0)| \tag{36}$$

$$\begin{aligned}\eta_{1,j}^n := &\int_{t^n}^{t^{n+1}} \int_{T_j} h_j |\partial_t \widetilde{u}_j + \nabla\cdot f(\widetilde{u}_j)| \\ &+ \frac{1}{2}\int_{t^n}^{t^{n+1}} \sum_{l\in N(j)} h_{jl} \int_{S_{jl}} Q_{jl}(\widetilde{u}_j, \widetilde{u}_l)|\widetilde{u}_j - \widetilde{u}_l| \\ &+ \int_{T_j} h_j |\widetilde{u}^n(t^n) - \widetilde{u}^{n-1}(t^n)|\end{aligned} \tag{37}$$

$$\begin{aligned}\eta_{2,j}^n := &\int_{t^n}^{t^{n+1}} \|\overline{\widetilde{u}_j^n} - \widetilde{u}_j^n\|_{L^\infty(T_j)} \int_{T_j} |\partial_t \widetilde{u}_j^n + \nabla\cdot f(\widetilde{u}_j^n)| \\ &+ \frac{1}{2}\int_{t^n}^{t^{n+1}} \sum_{l\in N(j)} \max_{k\in\{j,l\}} \|\overline{\widetilde{u}_k^n} - \widetilde{u}_k^n\|_{L^\infty(S_{jl})} \int_{S_{jl}} Q_{jl}(\widetilde{u}_j, \widetilde{u}_l)|\widetilde{u}_j - \widetilde{u}_l| \\ &+ \|\overline{\widetilde{u}^{n-1}}(t^n) - \widetilde{u}^{n-1}(t^n)\|_{L^\infty(T_j)} \int_{T_j} |\widetilde{u}^n(t^n) - \widetilde{u}^{n-1}(t^n)|\end{aligned} \tag{38}$$

Here, we used the following notation:

$$Q_{jl}(u,v) := \frac{2f_{jl}(u,v) - f_{jl}(u,u) - f_{jl}(v,v)}{u-v}, \quad h_{jl} := \operatorname{diam}(T_j \cup T_l)$$

The error estimator in Theorem 5.4 is composed of the two parts η_1, η_2. The first part corresponds to the standard estimates known for first-order schemes (see Theorem 3.4) and the second part of the estimate corresponds to error terms, which are only present in higher-order approximations.

For a further discussion on the error estimate and for the design of an *hp*-adaptive variant of the RK-DG method using this theoretical result, we refer to [18].

6. ADAPTIVE SCHEMES AND NUMERICAL EXPERIMENTS

In the sequel let us suppose that for some approximation u_h of the conservation law (1)–(2) or (16)–(18), we have an *a posteriori* error control of the following form:

$$|||u - u_h|||_K \leqslant \eta_h(u_h) \tag{39}$$

where the error indicators admit a localization in time and space as follows:

$$\eta_h(u_h) = \sum_{n\in I} \eta_h^n(u_h) \quad \text{and} \quad \eta_h^n(u_h) = \sum_{j\in J^n} \eta_j^n(u_h)$$

DOI: 10.1002/fld

Here $\eta_j^n(u_h)$ are supposed to be local error indicators that are assigned to the space–time segments $T_j^n \times [t^n, t^{n+1})$.

In the following subsection, we are going to describe an equal distribution strategy that can be used to design an efficient grid adaptive scheme.

6.1. Derivation of adaptive schemes from error control

The goal of an adaptive algorithm based on *a posteriori* error control is to choose the local grid size in such a way that

1. the computational cost is reduced or minimized and
2. the error $|||u-u_h|||_K$ is below some given tolerance TOL.

One possibility to obtain such an algorithm for a given tolerance TOL and some $\theta \in (0, 1)$ is the so-called equal distribution strategy. The principal idea of this strategy is to generate a mesh, such that the local contributions $\eta_j^n(u_h)$, $j \in J^n$ of the error estimator are approximately of the same size. Starting from a given mesh, this can be achieved either by moving mesh points (see [36]) or by successive refinement and coarsening of certain elements of a given mesh. Here, we will follow the second approach and define the method as follows:

Let a computational grid $\mathcal{T}^{n-1}$ and an approximation u_h^{n-1} on $\mathcal{T}^{n-1}$ at time t^{n-1} be given such that

$$\eta_h^{n-1}(u_h) \leqslant \frac{\Delta t^{n-1}}{T}\mathrm{TOL}$$

Compute $\mathcal{T}^n$ and an approximation u_h^n according to the following algorithm:

1. Set $\mathcal{T}^n = \mathcal{T}^{n-1}$.
2. Compute u_h^n, $\eta_h^n(u_h)$ on $\mathcal{T}^n$.
3. If $\eta_h^n(u_h) > \Delta t^n / T\,\mathrm{TOL}$, then

   (a) Refine or coarsen the grid locally such that for all $T_j \in \mathcal{T}^n$ it holds

   $$\eta_j^n(u_h) \leqslant \frac{\Delta t^n}{T|J^n|}\mathrm{TOL} \quad \text{and, if possible,} \quad \theta\frac{\Delta t^n}{T|J^n|}\mathrm{TOL} \leqslant \eta_j^n(u_h)$$

   This results in an updated grid $\mathcal{T}^n$.

   (b) Compute u_h^n, $\eta_h^n(u_h)$ on the adapted grid $\mathcal{T}^n$ and proceed with step 3.

   Else proceed with time step t^{n+1}.

If the computational grid is adapted according to the given algorithm, the local upper bounds of the indicators ensure that in the end

$$\eta_h(u_h) = \sum_{n\in I}\sum_{j\in J^n}\eta_j^n(u_h) \leqslant \sum_{n\in I}\sum_{j\in J^n}\frac{\Delta t^n}{T|J^n|}\mathrm{TOL} = \mathrm{TOL}$$

and thus the error $|||u-u_h|||_K$ is bounded by the tolerance TOL because of the *a posteriori* error estimate (39). The local lower bounds of the indicators, on the other hand, ensure that elements are coarsened if possible, thus leading to a minimal number of overall mesh cells.

DOI: 10.1002/fld

The refinement of elements is usually done by subdivision into smaller elements, e.g. bisection of elements or subdivision into congruent subelements. Coarsening, on the other hand, is usually the inverse of refinement and thus can only be performed for elements that were refined in a previous step. For our simulation we used the DUNE software package that supports such local mesh refinement *via* an abstract grid interface [37, 38].

Modifications and improvements of this algorithm to the approximation schemes discussed in the previous sections can be found in [3, 17, 18]. In particular, the performance of the algorithm can be improved if one first subdivides the elements into a significant set $\mathscr{T}_s^n$ and the complement $\mathscr{T}^n \setminus \mathscr{T}_s^n$ in such a way that $\mathscr{T}_s^n$ collects the elements with the largest indicator values, such that the sum of the error indicators corresponding to the elements in $\mathscr{T}_s^n$ is a prescribed percentage (e.g. 99%) of the overall indicator value $\eta^n(u_h)$. Thus, $\mathscr{T}_s^n$ contains all elements that significantly contribute to the overall error. The equal distribution strategy is then applied to the set $\mathscr{T}_s^n$ only. On the other hand, elements in the complement $\mathscr{T}^n \setminus \mathscr{T}_s^n$ are marked for coarsening. This strategy is for instance advantageous for applications, where the solution is constant within certain regions of the computational domain. A detailed description of this modification is described in [18] and applied in the simulations corresponding to test problems two and three in the following section.

In [18] it is also discussed how the local choice of the polynomial degree of the approximate solutions can be chosen with the help of the *a posteriori* error estimate given in Theorem 5.4. In examples two and three in the following section, we used this adaptive choice of the polynomial degree and we denote by $p_{\max}$ the maximum polynomial degree that was used in the simulation.

6.2. Numerical experiments

In this subsection we give some numerical experiments that underline the benefits that we get from adaptive methods resulting from the *a posteriori* error estimates. The first experiment is a linear transport problem on a two-dimensional bounded domain where the discretization and theoretical results presented in Section 4 were used. The second example is the Buckley–Leverett problem in one space dimension discretized with the discontinuous Galerkin method given in Section 5. Finally, the third example is the solid body rotation with a slotted disk, a cone and a smooth hump. As in the second example, the discontinuous Galerkin method from Section 5 was used for discretization.

6.2.1. First example: linear transport problem. As a first example we choose a linear problem where the inflow and outflow regions are known *a priori*. The example is chosen for instance as it comes with a known exact solution. Thus, we can compare the L^1-error between the exact and the approximate solution with the error estimator η_h defined in Theorem 4.4.

We look at the following initial boundary value problem in $\Omega := (0,1)\times(0,1)$:

$$u_t + \nabla\cdot(\mathbf{b}u) = 0 \quad \text{in } \Omega\times(0,T)$$

$$u(\cdot,0) = 0 \quad \text{in } \Omega$$

$$u(x,t) = \overline{u}(t,x) \quad \text{in } \partial\Omega\times(0,T)$$

Then $u(x,t)$ is constant along the streamlines of the prescribed velocity field $\mathbf{b}(x_1,x_2) := (x_2,-x_1)^\top$ and therefore depends only on the initial data, and on the boundary values at the inflow boundary.

DOI: 10.1002/fld

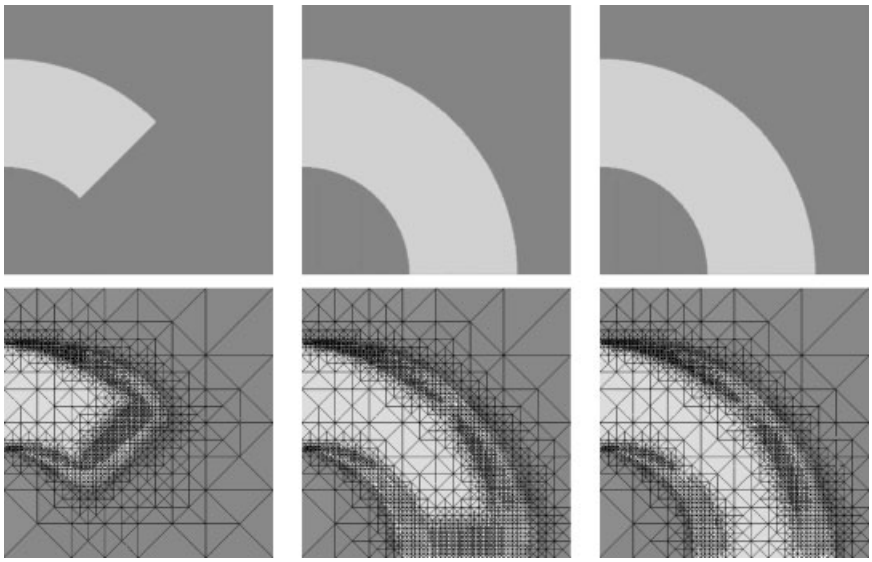

Figure 3. Color shading of the exact solution of the linear problem at $t=\pi/4, \pi/2,$ and $t=2$ (top row) and adaptive solution of the linear problem at the same times (bottom row). A color shading of the solution together with the adaptive grid is plotted for the full upwind flux.

In our example we set

$$\overline{u}(t,x) := \begin{cases} 1 & \text{if } x \in \{0\} \times (0.4, 0.8) \\ 0 & \text{else} \end{cases}$$

The exact solution for several times is depicted in the top row of Figure 3.

We analyze the performance of the adaptive scheme *versus* the same scheme on a mesh with uniform mesh size. Therefore, in Figure 4 we plot the L^1 error *versus* run time for uniform and adaptive computations using the upwind flux. The comparison shows that the adaptive scheme performs much better than the method on uniform grids. In addition, we stress that the adaptive algorithm requires far less storage than the uniform one. For instance, in the finest computations, the maximal number of mesh cells in the adaptive case was about 350 000, while 4 200 000 mesh cells were used in the uniform computation. An approximate solution on an adaptive grid is given in the bottom row of Figure 3.

6.2.2. Second example: Buckley–Leverett problem. As a second example we look at the Buckley–Leverett equation, which is a one-dimensional model for two-phase flow in porous media where capillary pressure effects are neglected. The unknown variable $u : (-1, 1) \times (0, 0.4) \to \mathbb{R}$ is the saturation of the wetting phase within a two-phase mixture. It satisfies the non-linear conservation law

$$u_t + \partial_x f(u) = 0 \quad \text{on } (-1,1) \times (0, 0.4), \qquad u(\cdot, 0) = u_0 \quad \text{on } (-1, 1)$$

DOI: 10.1002/fld

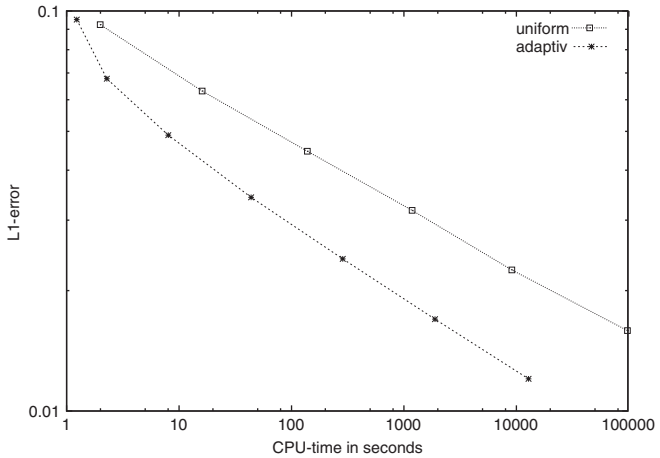

Figure 4. L^1 error *versus* run time for uniform and adaptive computations for the linear problem.

where the fractional flow rate f is given as $f(s)=u^2/(u^2+\frac{1}{2}(1-u)^2)$. We look at the Cauchy problem with the following initial data:

$$u_0(x) := \begin{cases} 0 & \text{for } x \in (-0.6, 0.2) \\ 1 & \text{else} \end{cases}$$

Thus, the solution of our Buckley–Leverett problem consists of the solution of two distinct Riemann problems for t smaller than some critical time $T^*>0.4$. The solution of each Riemann problem is a composed wave consisting of a rarefaction wave and an attached shock.

In Figure 5 we plot the exact solution together with the approximation using our adaptive strategy for $p_{\max}=1, 2$ and $\mathrm{TOL}=0.25$ and 0.125. Since the structure of the solution away from the discontinuities is very simple, the advantage of the quadratic Ansatz functions ($p_{\max}=2$) is not evident. The grid density function hardly depends on the polynomial degree since almost all grid points are located in the shock regions. Only the kinks at the beginning of the rarefaction waves lead to additional slight refinement. Since the highest grid resolution produced by our refinement strategy is the same for $p_{\max}=1$ and 2 and the approximation error is dominated by the shocks, the $p_{\max}=2$ version of the DG method does not lead to a more efficient scheme as can be seen from Figure 6 where the error is plotted over M_{tot}, the overall number of mesh cells, summed over all time steps. A more complicated structure of the solution—as can only be found in systems in higher space dimension—is required to demonstrate the advantage of a *hp*-adaptive strategy for non-linear conservation laws with discontinuous solutions.

6.2.3. Third example: solid body rotation. As a third example we choose the solid body rotation introduced in [39, 40]. In order to be comparable to [39], we choose a smooth hump, a cone, and a slotted disk as solid bodies that are rotated with constant angular speed, i.e. $\mathbf{b}(x_1, x_2) := (-x_2, x_1)^\top$ in $\Omega := [-1, 1]^2$. The initial data are plotted in Figure 7(a). For a detailed description of this model problem, we refer to [39].

DOI: 10.1002/fld

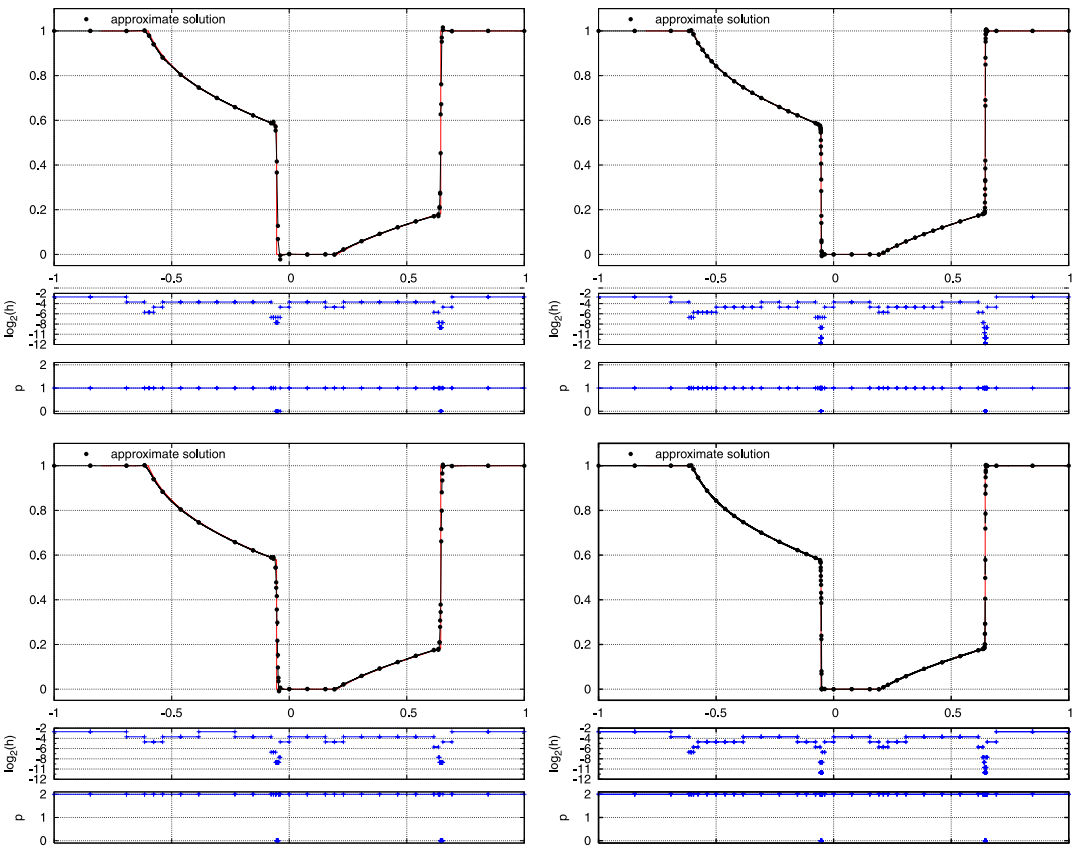

Figure 5. Comparison of the approximate solutions obtained with the discontinuous Galerkin method for $p_{\max}=1$ (top row) and $p_{\max}=2$ (bottom row) with TOL$=0.25$ (left-hand side) and TOL$=0.125$ (right-hand side) on adaptively refined grids. The approximate solutions are compared with the exact solution (solid line) at $T=0.4$. The local mesh size h of the adaptive grid and the distribution of the local polynomial degree p are plotted in the middle and bottom row, respectively.

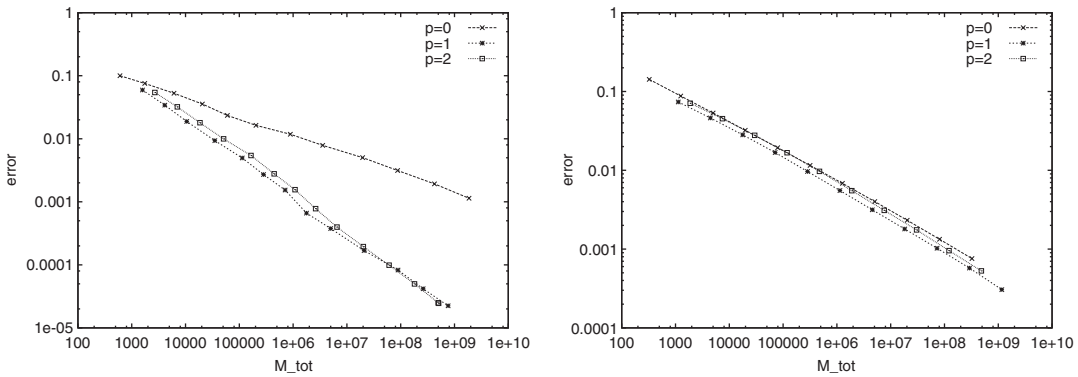

Figure 6. Convergence study for the discontinuous Galerkin method on adaptively refined grids (left) and uniform refined grids (right) for $p_{\max}=0,1,2$.

DOI: 10.1002/fld

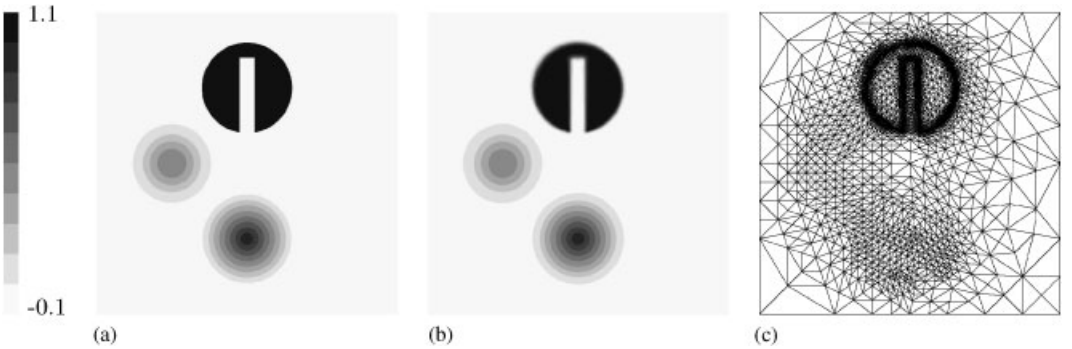

Figure 7. Simulation result for the solid body rotation. The plots show the exact initial data (a), the simulation result after one rotation with TOL$=0.15$ (b) and the adaptive computational grid after one rotation (approximately 8000 elements) (c).

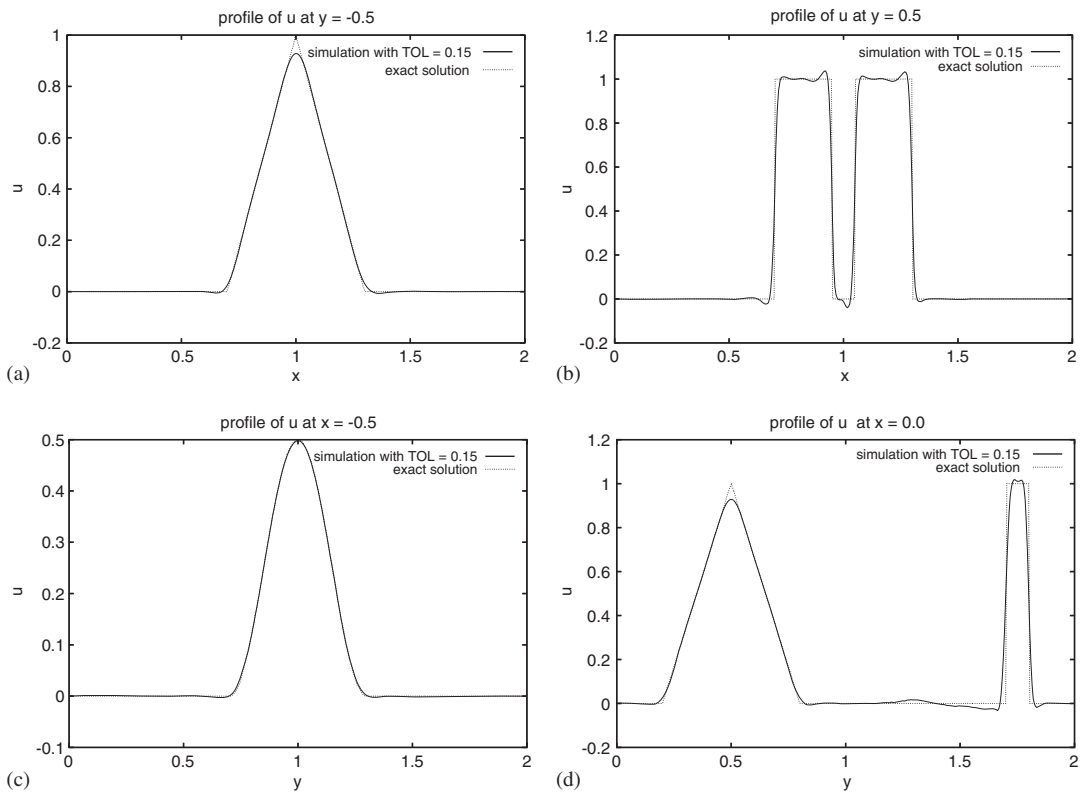

Figure 8. Simulation result for the solid body rotation with TOL$=0.15$. The plots show different cross sections of the approximate solution in comparison with the exact profiles at $y=-0.5$ (a), $y=0.5$ (b), $x=-0.5$ (c), and $x=0.0$ (d).

DOI: 10.1002/fld

TOL	elements at $t = T$	average Δt	L^1 error at $t = T$
0.600	884	0.00268	0.0853
0.300	2115	0.00148	0.0529
0.150	7986	0.00060	0.0286
0.075	18893	0.00028	0.0162

(a)

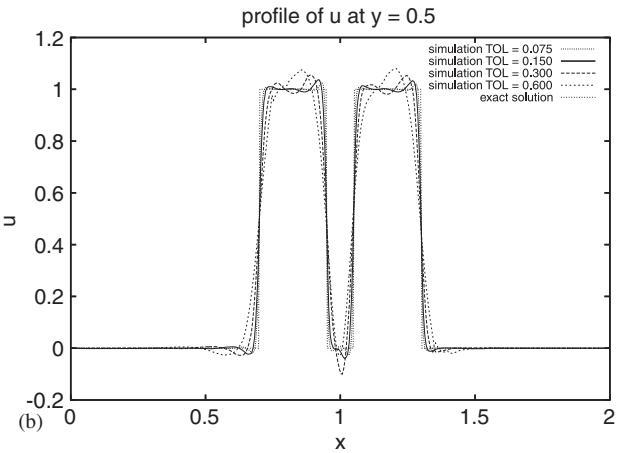

(b)

Figure 9. Table (a) shows the dependence of the number of elements, the average time step size and the L^1 error on the value of the prescribed tolerance TOL for the third example. Plot (b) shows the approximate solutions for TOL$=0.60$, 0.30, 0.15, and 0.75 on a cross section at $y=0.5$ together with the exact solution.

In Figure 7 we plotted the numerical result for the adaptive DG method, using $p_{\max}=2$. The tolerance is chosen such that the adaptive scheme resolves the bodies with about 8000 triangles. Thus, the size of the computational mesh is comparable to the size of the uniform structured mesh that was used in [39].

The approximate solution after one rotation for TOL$=0.15$ is plotted in Figure 7(b), while the corresponding adaptively refined mesh is plotted in Figure 7(c). The distribution of the elements shows that most of the computational costs is due to the resolution of the slotted disk, while only moderate refinement is needed to resolve the cone and the smooth hump. In Figure 8 the solution for TOL$=0.15$ is further analyzed. The plots (a)–(d) show the profile of the solution on cross sections corresponding to $y=-0.5$, $y=0.5$, $x=-0.5$, and $x=0.0$, respectively. In comparison with the numerical results obtained in [39], the adaptive method shows a very nice approximation of the exact solution with even less grid cells and an unstructured mesh. We also remark that the presented method allows for small oscillations around the discontinuous slotted disk. A study for varying tolerances in Figure 9(b), however, reveals that the oscillations decrease with smaller tolerances and the discontinuities get better and better resolved. Figure 9(a) shows the dependence of the adaptive approximation on the choice of the prescribed tolerance TOL.

The results so far show that our adaptive strategy based on the *a posteriori* error estimates from Theorems 4.4 and 5.4 leads to good schemes both for linear and non-linear test problems.

The application of the adaptive technology presented here to systems of conservation laws is certainly not possible on the theoretical level as our approach makes use of at least one parameter family of entropy solutions. On the other hand, it is certainly possible to advise adaptive numerical schemes also for systems, based on the scalar ideas. Such investigations are under consideration and will be addressed in further contributions.

DOI: 10.1002/fld

7. FURTHER RESULTS AND DISCUSSION OF THE LITERATURE

In this section we give some references to further results and approaches concerning *a posteriori* error control and adaptivity for hyperbolic conservation laws.

In the framework of the doubling of variables technique, we wish to especially refer to the work of Makridakis *et al.* [20, 41, 42] where similar results to those presented in Section 3 were obtained for MUSCL finite difference schemes in one space dimension and for finite volume relaxation schemes. For staggered Lax Friedrichs schemes on general unstructured meshes, a corresponding *a posteriori* result was obtained by Küther (see [43, 44]).

A different approach towards *a posteriori* error control is the usage of the Oleinik entropy condition instead of the Kruzkov framework. This leads to stability results that can be exploited in the analysis of the dual problem of the underlying conservation laws. Unfortunately, this approach is restricted to one space dimension. For results in this direction, we refer to the pioneering work of Tadmor [45] for finite difference approximations and to the article of Johnson and Szepessy [33] for the analysis of finite element approximations.

A posteriori error estimates in negative norms (e.g. H^{-1}) were derived by Houston *et al.* for approximations of scalar conservation laws and Friedrichs systems (see [46–48]). An *a posteriori* error estimate for finite volume approximations of weak solutions of Friedrichs systems was recently given by Jovanovic and Rohde [49].

The literature on *a posteriori* error control and adaptive solution algorithms for RK–DG approximations is rare. We refer for instance to the articles of Hartmann and Houston [50] and Larson and Barth [51] where duality techniques were used for designing adaptive schemes. We also refer to Houston *et al.* [52–54] for *hp*-adaptive DG methods for hyperbolic problems. Another approach towards error control for DG methods was introduced by Adjerid *et al.* [55] where asymptotically correct *a posteriori* estimates of spatial discretization errors were derived in one dimension for smooth solutions.

Last but not the least, using compression algorithms from wavelet theory, efficient adaptive multiscale finite volume methods for conservation laws were derived by Müller *et al.* [56, 57].

ACKNOWLEDGEMENTS

We thank the anonymous referees for their useful comments to improve this presentation.

REFERENCES

1. Kruzkov SN. First order quasilinear equations in several independent variables. *Mathematics of the USSR—Sbornik* 1970; **10**:217–243.
2. Kuznetsov NN. Accuracy of some approximate methods for computing the weak solutions of a first-order quasi-linear equation. *USSR Computational Mathematics and Mathematical Physics* 1976; **16**(6):159–193.
3. Kröner D, Ohlberger M. A posteriori error estimates for upwind finite volume schemes for nonlinear conservation laws in multi dimensions. *Mathematics of Computation* 2000; **69**:25–39.
4. Vol'pert AI, Hudjaev SI. Cauchy's problem for degenerate second order quasilinear parabolic equations. *Mathematics of the USSR—Sbornik* 1969; **7**(3):365–387.
5. Gallouët T, Herbin R. A uniqueness result for measure-valued solutions of nonlinear hyperbolic equations. *Differential and Integral Equations* 1993; **6**(6):1383–1394.
6. Otto F. Initial-boundary value problem for a scalar conservation law. *Comptes Rendus de l Academie des Sciences Paris, Série I—Mathematique* 1996; **322**(8):729–734.

DOI: 10.1002/fld

7. Vovelle J. Convergence of finite volume monotone schemes for scalar conservation laws on bounded domains. *Numerische Mathematik* 2002; **90**(3):563–596.
8. Vila JP. Convergence and error estimates in finite volume schemes for general multi-dimensional scalar conservation laws. I. Explicit monotone schemes. *RAIRO—Modélisation Mathematique et Analyse Numérique* 1994; **28**: 267–295.
9. Cockburn B, Coquel F, Lefloch PG. An error estimate for finite volume methods for multidimensional conservation laws. *Mathematics of Computation* 1994; **63**:77–103.
10. Eymard R, Gallouët T, Ghilani M, Herbin R. Error estimates for the approximate solution of a nonlinear hyperbolic equation given by finite volume schemes. *IMA Journal of Numerical Analysis* 1998; **18**:563–594.
11. Cockburn B, Gremaud PA. A priori error estimates for numerical methods for scalar conservation laws. Part I: the general approach. *Mathematics of Computation* 1996; **65**:533–573.
12. Cockburn B, Gremaud PA. A priori error estimates for numerical methods for scalar conservation laws. Part 2: flux splitting montone schemes on irregular Cartesian grids. *Mathematics of Computation* 1996; **66**:547–572.
13. Cockburn B, Gremaud PA, Yank JX. A priori error estimates for numerical methods for scalar conservation laws. Part III: multidimensional flux-splitting monotone schemes on non-Cartesian grids. *Mathematics of Computation* 1996; **65**:533–573.
14. Eymard R, Galluoët T, Herbin R. Finite volume methods. In *Handbook of Numerical Analysis*, vol. VII. North-Holland: Amsterdam, 2000; 713–1020.
15. Chainais-Hillairet C. Finite volume schemes for a nonlinear hyperbolic equation. Convergence towards the entropy solution and error estimates. *Mathematical Modelling and Numerical Analysis* 1999; **33**:129–156.
16. Cockburn B, Gau H. A posteriori error estimates for general numerical methods for scalar conservation laws. *Computational and Applied Mathematics* 1995; **14**:37–47.
17. Ohlberger M, Vovelle J. Error estimate for the approximation of non-linear conservation laws on bounded domains by the finite volume method. *Mathematics of Computation* 2006; **75**:113–150.
18. Dedner A, Makridakis C, Ohlberger M. Error control for a class of Runge–Kutta discontinuous Galerkin methods for nonlinear conservation laws. *SIAM Journal on Numerical Analysis* 2007; **45**(2):514–538.
19. Bouchut F, Perthame B. Kruzkov's estimates for scalar conservation laws revisited. *Transactions of the American Mathematical Society* 1998; **350**(7):2847–2870.
20. Katsoulakis MA, Kossioris G, Makridakis Ch. Convergence and error estimates of relaxation schemes for multidimensional conservation laws. *Communications in Partial Differential Equations* 1999; **24**(3–4):395–424.
21. Szepessy A. Convergence of a streamline diffusion finite element method for scalar conservation laws with boundary conditions. *RAIRO—Modélisation Mathematique et Analyse Numérique* 1991; **25**(6):749–782.
22. Benharbit S, Chalabi A, Vila JP. Numerical viscosity and convergence of finite volume methods for conservation laws with boundary conditions. *SIAM Journal on Numerical Analysis* 1995; **3**:775–796.
23. Cockburn B, Coquel F, LeFloch PG. Convergence of the finite volume method for multidimensional conservation laws. *SIAM Journal on Numerical Analysis* 1995; **32**(3):687–705.
24. Bardos C, LeRoux AY, Nédélec J-C. First order quasilinear equations with boundary conditions. *Communications in Partial Differential Equations* 1979; **4**(9):1017–1034.
25. Málek J, Nečas J, Rokyta M, Ružička M. *Weak and Measure-valued Solutions to Evolutionary PDEs*. Chapman & Hall: London, 1996.
26. Serre D. *Systèmes de lois de conservation. II*. Diderot Editeur: Paris, 1996. Structures géométriques, oscillation et problèmes mixtes (Geometric structures, oscillation and mixed problems).
27. Carrillo J. Entropy solutions for nonlinear degenerate problems. *Archive for Rational Mechanics and Analysis* 1999; **147**(4):269–361.
28. Vignal MH. Schemas Volumes Finis pour des equations elliptiques ou hyperboliques avec conditions aux limites, convergence et estimations d'erreur. *Thesis*, L'Ecole Normale Superieure, Lyon, 1997.
29. Cockburn B, Shu C-W. Runge–Kutta discontinuous Galerkin methods for convection-dominated problems. *Journal of Scientific Computing* 2001; **16**(3):173–261.
30. Cockburn B, Shu C-W. TVB Runge–Kutta local projection discontinuous Galerkin finite element method for conservation laws. II. General framework. *Mathematics of Computation* 1989; **52**(186):411–435.
31. Zhang Q, Shu C-W. Error estimates to smooth solutions of Runge–Kutta discontinuous Galerkin methods for scalar conservation laws. *SIAM Journal on Numerical Analysis* 2004; **42**(2):641–666.
32. Jaffré J, Johnson C, Szepessy A. Convergence of the discontinuous Galerkin finite element method for hyperbolic conservation laws. *Mathematical Models and Methods in Applied Sciences* 1995; **5**(3):367–386.
33. Johnson C, Szepessy A. Adaptive finite element methods for conservation laws based on a posteriori error estimates. *Communications on Pure and Applied Mathematics* 1995; **48**:199–234.

DOI: 10.1002/fld

34. Cockburn B, Gremaud PA. Error estimates for finite element methods for scalar conservation laws. *SIAM Journal on Numerical Analysis* 1996; **33**:522–554.
35. Dedner A, Ohlberger M. A new *hp*-adaptive dg scheme for conservation laws based on error control. In *Proceedings of the 11th International Conference on Hyperbolic Problems*, Lyon, 17–21 July 2006, Benzoni-Gavage S, Serre D (eds). Hyperbolic Problems: Theory, Numerics, Applications. Springer: Berlin, 2008.
36. Tang T. Moving mesh methods for computational fluid dynamics. *Recent Advances in Adaptive Computation*, *Contemporary Mathematics*, vol. 383. American Mathematical Society: Providence, RI, 2005; 141–173.
37. DUNE—Distributed and Unified Numerics Environment. http://dune-project.org/.
38. Bastian P, Droske M, Engwer C, Klöfkorn R, Neubauer T, Ohlberger M, Rumpf M. Towards a unified framework for scientific computing. *Proceedings of the 15th International Conference on Domain Decomposition Methods*, Berlin, 21–25 July 2003.
39. Leveque RJ. High-resolution conservative algorithms for advection in incompressible flow. *SIAM Journal on Numerical Analysis* 1996; **33**(2):627–665.
40. Zalesak ST. Fully multidimensional flux-corrected transport algorithms for fluids. *Journal of Computational Physics* 1979; **31**(3):335–362.
41. Gosse L, Makridakis C. Two a posteriori error estimates for one-dimensional scalar conservation laws. *SIAM Journal on Numerical Analysis* 2000; **38**(3):964–988.
42. Katsaounis T, Makridakis C. Finite volume relaxation schemes for multidimensional conservation laws. *Mathematics of Computation* 2001; **70**(234):533–553.
43. Küther M. Error estimates for the staggered Lax Friedrichs scheme on unstructured grids. *SIAM Journal on Numerical Analysis* 2001; **39**(4):1269–1301.
44. Küther M, Ohlberger M. Adaptive second order central schemes on unstructured staggered grids. In *Hyperbolic Problems*: *Theory*, *Numerics*, *Applications. Proceedings of the 9th International Conference on Hyperbolic Problems*, Pasadena, 2002, Hou TY, Tadmor E (eds). Springer: Berlin, 2003.
45. Tadmor E. Local error estimates for discontinuous solutions of nonlinear hyperbolic equations. *SIAM Journal on Numerical Analysis* 1991; **28**:891–906.
46. Süli E, Houston P. Finite element methods for hyperbolic problems: a posteriori error analysis and adaptivity. *The State of the Art in Numerical Analysis*, New York, 1996, The Institute of Mathematics and its Applications Conference Serie, New Series, vol. 63. Oxford University Press: New York, 1997; 441–471.
47. Houston P, Mackenzie JA, Süli E, Warnecke G. A posteriori error analysis for numerical approximation of Friedrichs system. *Numerische Mathematik* 1999; **82**(3):433–470.
48. Warnecke G. Adaption and reliability of numerical methods for stiff and nonstiff problems in CFD. *Computational Fluid Dynamics* 2000; **9**(1).
49. Jovanović V, Rohde C. Finite-volume schemes for Friedrichs systems in multiple space dimensions: a priori and a posteriori error estimates. *Numerical Methods for Partial Differential Equations* 2005; **21**(1):104–131.
50. Hartmann R, Houston P. Adaptive discontinuous Galerkin finite element methods for nonlinear hyperbolic conservation laws. *SIAM Journal on Scientific Computing* 2002; **24**(3):979–1004.
51. Larson MG, Barth TJ. A posteriori error estimation for adaptive discontinuous Galerkin approximations of hyperbolic systems. *Discontinuous Galerkin Methods*, Lecture Notes in Computational Science and Engineering, Newport, RI, 1999, vol. 11. Springer: Berlin, 2000; 363–368.
52. Houston P, Süli E. *hp*-adaptive discontinuous Galerkin finite element methods for first-order hyperbolic problems. *SIAM Journal on Scientific Computing* 2001; **23**(4):1226–1252.
53. Houston P, Senior B, Süli E. *hp*-discontinuous Galerkin finite element methods for hyperbolic problems: error analysis and adaptivity. *International Journal for Numerical Methods in Fluids* 2002; **40**(1–2):153–169 (ICFD Conference on Numerical Methods for Fluid Dynamics, Oxford, 2001).
54. Süli E, Houston P. Adaptive finite element approximation of hyperbolic problems. *Error Estimation and Adaptive Discretization Methods in Computational Fluid Dynamics*, Lecture Notes in Computational Science and Engineering, vol. 25. Springer: Berlin, 2003; 269–344.
55. Adjerid S, Devine KD, Flaherty JE, Krivodonova L. A posteriori error estimation for discontinuous Galerkin solutions of hyperbolic problems. *Computer Methods in Applied Mechanics and Engineering* 2002; **191**(11–12):1097–1112.
56. Cohen A, Kaber SM, Müller S, Postel M. Fully adaptive multiresolution finite volume schemes for conservation laws. *Mathematics of Computation* 2003; **72**(241):183–225.
57. Müller S. *Adaptive Multiscale Schemes for Conservation Laws*. Lecture Notes in Computational Science and Engineering, vol. 27. Springer: Berlin, 2003.

DOI: 10.1002/fld